A Novel Biopolymer-based Nanomagnetic Catalyst for the Synthesis of 4*H*-pyran and Tetrahydro-4*H*-chromene Derivatives

Amin Mohammadzadeh[a], Ahmad Poursattar Marjani[a,*] [§] and Asghar Zamani[b]

[a]*Department of Organic Chemistry, Faculty of Chemistry, Urmia University, Urmia, Iran.*
[b]*Department of Nanotechnology, Faculty of Science, Urmia University, Urmia, Iran.*

Received 24 October 2019, revised 26 March 2020, accepted 13 April 2020.

ABSTRACT

In the present study, we have designed and synthesized a new magnetically recoverable, nanocatalyst of Ag/Fe_3O_4@starch. The successful synthesis and the structure of the nanocatalyst were confirmed and evaluated with several analytical techniques including XRD, EDX, VSM, FT-IR, TEM and TGA. The impact and efficiency of Ag/Fe_3O_4@starch were successfully investigated in the one-pot synthesis of desired 4*H*-pyrans and tetrahydro-4*H*-chromenes using three-component condensation of various aldehydes, malononitrile, and 1,3-diketoesters or cyclic 1,3-diketones. The magnetic nanocatalyst was easily recovered and reused with high catalytic activity even after up to five runs.

KEYWORDS

Green synthesis, nanomagnetic, reusable nanocatalyst, starch, 4*H*-pyrans, tetrahydro-4*H*-chromenes.

1. Introduction

Green chemistry is a developing field of sustainable sciences and technologies that aids in the use of renewable feedstock as sustainable resources. Biopolymers such as starch, chitosan and cellulose, are extracted from biomass and have recyclability and reusability comparable with traditional synthetic polymers.[1] Among these green polymers, starch is well known because of its abundance and low cost when extracted from agricultural products.[2] One of the applications of native starch is as a sizing agent; however, further modifications can change its properties to be used as a film-forming agent owing to its outstanding coating property.[3] Starch may be commercially obtained from numerous vegetal feedstock (seeds, roots and tubers) such as cornstarch, arrowroot, tapioca, wheat, rice and potato. In recent years, starch has achieved great attention as green and inexpensive support, stabilizer and reducing agent in the synthesis of metal nanoparticles.[4] It is excellent in forming metal complexes due to the numerous hydroxyl groups present within the starch structure, allowing for control of size, shape, and dispersivity of metal nanoparticles in starch. Various reports have been made in the literature regarding the starch-stabilized synthesis of nanoparticles, such as silver,[5] gold[6] and palladium.[7]

The use of magnetic nanoparticles (MNPs) has recently become important because of their potential use in medicinal fields, catalysis, microfluidics, biomedicine, magnetic resonance imaging, and data storage.[8] Fe_3O_4 MNPs have been employed as an outstanding solid catalyst in organic processes,[9] due to their high surface area, easy synthesis and handling, simple recoverability, oxidative stability and nontoxicity. Fe_3O_4 MNPs can be synthesized by several methods, although co-precipitation is the most common technique.[10] In this technique, MNPs are prepared using Fe(II) and Fe(III) ions in basic solution under an inert atmosphere.

The polyfunctionalized 4*H*-pyran and tetrahydro-4*H*-chromene moieties are among significant heterocyclic compounds that contain oxygen atoms, that exhibit the broad range of biological activities such as antimicrobial, anticarcinogen, a blood thinner, anti-anaphylactic anti-Parkinson, and anti-Alzheimer properties.[11]

4*H*-pyran and tetrahydro-4*H*-chromene derivatives can be synthesized with a three-component process of aldehydes, malononitrile and a compound with an active methylene group, 1,3-diketoesters or cyclic 1,3-diketones, under several conditions in the presence of a wide range of catalysts.[12]

As part of our ongoing attempts at using biopolymer-based catalysts,[13] in this work, it was shown that silver supported on Fe_3O_4/starch nanocomposite (Ag/Fe_3O_4@starch), significantly improves the catalytic performance in a three-component reaction of cyclic 1,3-diketones/1,3-diketoesters, aldehydes, and malononitrile in respect of synthesizing tetrahydro-4*H*-chromene derivatives. The prepared catalysts were investigated with X-ray diffraction (XRD), energy-dispersive X-ray spectrometry (EDX), vibrating sample magnetometry (VSM), Fourier-transform infrared (FT-IR) spectrometry, transmission electron microscopy (TEM) and thermogravimetric analysis (TGA) techniques. The successful nanocatalyst preparation was confirmed. Furthermore, different starting materials were used to evaluate the efficiency of the synthesized nanocatalysts and high yields were obtained. The reusability, as a substantial factor in catalyst design, was investigated for the prepared nanocatalyst. The nanocatalysts were reused in five cycles with no significant activity loss observed.

2. Experimental

2.1. Materials and Methods

All chemical materials needed were purchased from Acros, Fluka and Merck companies and no further purification processes were carried out on any of the chemicals. Thin-layer chromatography (TLC) silica gel on an aluminium plate was used to monitor the progress of the reactions. A Philip Harris

* To whom correspondence should be addressed.
E-mail: a.poursattar@urmia.ac.ir / a.poursattar@gmail.com

ISSN 0379-4350 Online / ©2020 South African Chemical Institute / http://saci.co.za/journal
DOI: https://doi.org/10.17159/0379-4350/2020/v73a9

C4954718 apparatus was applied for melting point measurements with no data correction. Infrared, ^{1}H NMR and ^{13}C NMR spectra of the synthesized materials were obtained with Thermo Nicolet Nexus 670 FT-IR spectrophotometer and Bruker Avance AQS 300 MHz spectrometer, respectively. DMSO-d_6 and TMS were used as a solvent and internal standard in NMR spectra recording respectively. XRD patterns were achieved with a JEOL JDX–8030 (30 kV, 20 mA). TGA and DTA thermograms were obtained with STA504 instrument. Magnetic properties of the nanocomposites were evaluated using a Lake Shore VSM 7410. Isolation and identification of the products were accomplished by comparing the obtained spectral data with reliable samples. TEM analysis was provided with an instrument CM30, Philips.

2.2. Cross-linking of Starch

2 g of Starch was dissolved in water (50 mL). Citric acid (0.4 g) and sodium hypophosphite (0.2 g) were added. The obtained dispersion was heated up to 90 °C under reflux conditions for 2 h. The mixture was cooled down to room temperature, and the precipitate was filtered and dried for one day in the oven at 40–50 °C. Finally, the product was crushed and powdered followed by washing with cold water several times. The resultant cross-linked starch was dried in an oven at 40–50 °C.

2.3. Preparation of Magnetic Ag/Fe_3O_4@starch Nano Biocomposites

The cross-linked starch (1 g) and 50 mL of water were mixed and the resultant mixture was warmed up to 80 °C until the starch had gelatinized. The heated starch solution was cooled down to room temperature. Then, 2.3 g of $FeCl_3.6H_2O$ and 0.75 g of $FeSO_4.7H_2O$ were dissolved in 25 mL water under vigorous agitation at room temperature. Thereafter, the solution was mixed drop by drop with the prepared gelatin starch for 10 min and the mixture was stirred at 80 °C. Then, NH_3 (25 %, 10 mL) was slowly added to the prepared solution and the resultant Fe_3O_4@starch was obtained by filtration after 20 min, following by rinsing with distilled water. The resultant product was dried and powdered. 1 g of powder was mixed in 35 mL water and 10 mL of 0.05 M $AgNO_3$ (aq.) was added. The resultant mixture was stirred at 90 °C for 30 min. Finally, the magnetic Ag/Fe_3O_4@starch nanocatalyst was rinsed several times using water and dried at 80 °C in an oven.

2.4. General Procedure for the Synthesis of 4*H*-pyran and Tetrahydro-4*H*-chromene Derivatives 4a–t

A mixture of aldehydes (1 mmol), malononitrile (1 mmol) and cyclic 1,3-diketones/1,3-diketoesters (1 mmol), and Ag/Fe_3O_4@starch (15 mg) in EtOH (5 mL) was warmed up to 50 °C over an appropriate time. The progress of the reaction was followed by TLC. The obtained mixture was cooled to room temperature and the solid material was filtered off and dissolved in hot EtOH. The catalyst was removed using a bar magnet and the precipitate was separated and crystallized from EtOH to give the desired products **4a–t** in 84–95 % yield.

Spectral Data for Selected Compounds

2-Amino-5-oxo-4-phenyl-5,6,7,8-tetrahydro-4*H*-chromene-3-carbonitrile (4k): white solid; 87 % (229 mg); M.p. 238–240 °C; IR ν_{max}: 3349, 3201 (NH_2), 2955, 2194 (CN), 1685 (C=O) cm^{-1}; δ_H (300 MHz, DMSO-d_6): 1.91–2.12 (2H, m, CH_2), 2.25–2.43 (2H, m, CH_2), 2.51–2.74 (2H, m, CH_2), 4.21 (1H, s, CH), 6.85 (2H, s, NH_2), 7.01–7.49 (5H, m, ArH) ppm; δ_C (75.5 MHz, DMSO-d_6): 20.66, 27.59, 36.49, 37.35, 58.93, 113.99, 120.46, 127.19, 127.69, 128.74, 145.46, 159.27, 165.50, 196.75.

2-Amino-5,6,7,8-tetrahydro-7,7-dimethyl-5-oxo-4-phenyl-4*H*-chromene-3-carbonitrile (4p): light yellow solid; 92 % (270 mg); M.p. 229–231 °C; IR ν_{max}: 3394, 3323 (NH_2), 2963, 2882, 2198 (CN), 1661 (C=O) cm^{-1}; δ_H (300 MHz, DMSO-d_6): 0.94 (3H, s, CH_3), 1.02 (3H, s, CH_3), 2.05–2.21 (2H, m, CH_2), 2.57 (2H, s, CH_2), 4.16 (1H, s, CH), 6.87 (2H, s, NH_2), 6.75–6.97 (3H, m, ArH), 6.98–7.26 (2H, m, ArH) ppm; δ_C (75.5 MHz, DMSO-d_6): 27.51, 31.81, 34.78, 38.96, 49.67, 58.28, 112.70, 119.71, 127.29, 128.16, 129.32, 144.78, 158.51, 162.46, 195.63 ppm.

3. Results and Discussion

3.1. FT-IR Spectroscopy

The FT-IR spectroscopy was used to study and confirm the successful preparation of the cross-linked starch and nanoparticle loaded magnetic nanocatalysts. In this respect, cross-linked and non-cross-linked starch are presented in Fig. 1a, and Fig. 1b, respectively.

The two spectra have similar FT-IR pattern, except the peak in the cross-linked starch at 1736 cm^{-1}, which is related to the carboxyl and ester carbonyl bands. Fig. 1c, shows the FT-IR spectrum of Fe_3O_4@starch. The appearance of a peak at 576 cm^{-1} corresponds to O-Fe bond vibration. Addition of $AgNO_3$ to a hot aqueous mixture of magnetic nanocomposite resulted in Fe_3O_4@starch stabilized silver, Ag/Fe_3O_4@starch *via* reduction of silver ions by hydroxyl groups in starch. The structural changes because of the interaction between Fe_3O_4@starch and silver species were studied by using FT-IR spectra (Fig. 1d). The shift at 3415 and 1635 cm^{-1} bands (Fig. 1c) to a lower wavelength at 3393 and 1631 cm^{-1} in the presence of Ag (Fig. 1d) was possibly due to the coordination of Ag with the hydroxyl groups in Fe_3O_4@starch.

3.2. XRD Spectroscopy

To investigate the structure of synthesized nanocatalyst, XRD was used. Fig. 2, shows the XRD pattern of Ag/Fe_3O_4@starch.

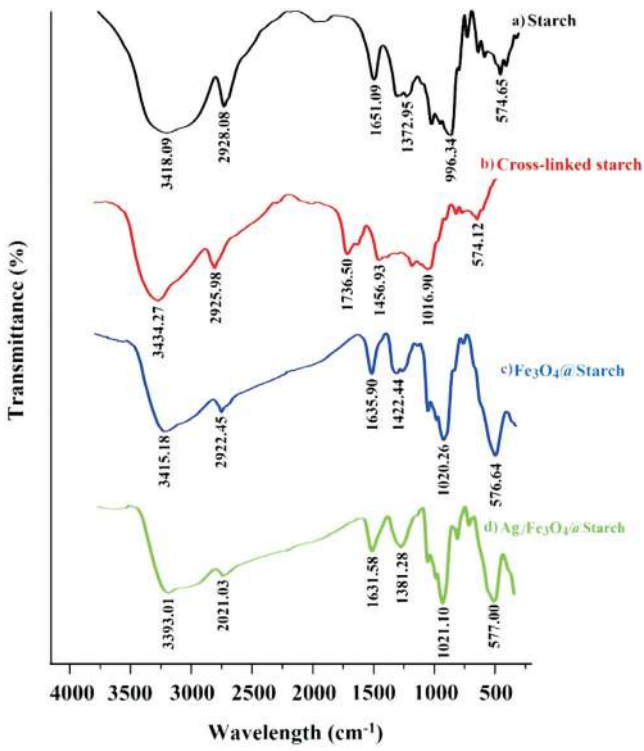

Figure 1 Near FT-IR spectra of potato starch (a), cross-linked starch (b), Fe_3O_4@starch (c) and Ag/Fe_3O_4@starch (d).

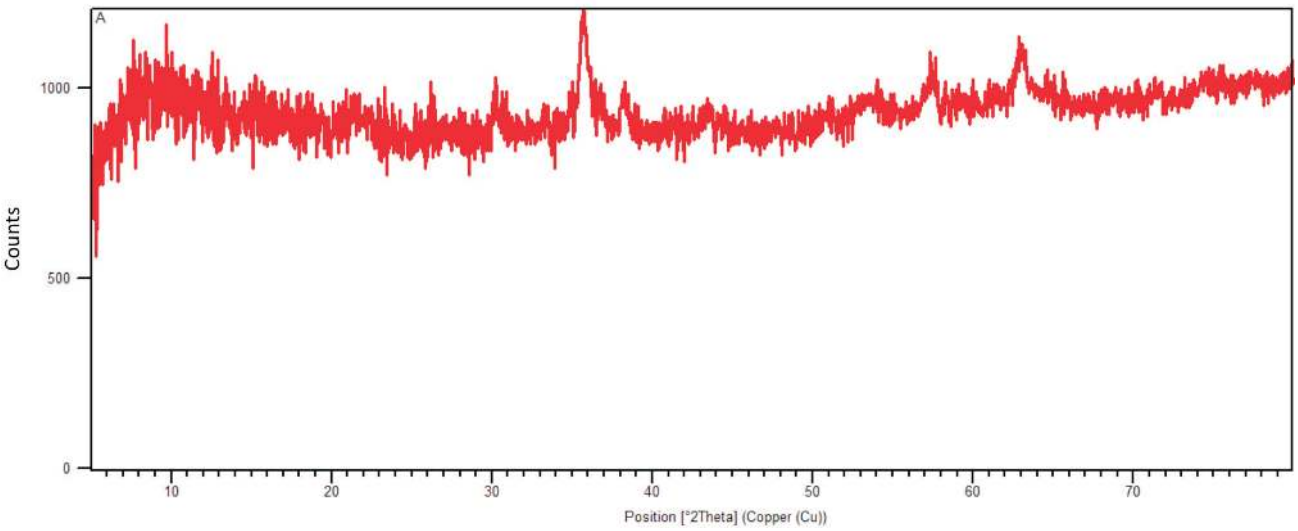

Figure 2 XRD pattern of Ag/Fe_3O_4@starch nanocomposite.

The peaks at $2\theta = 35.7\,°$ and $62.9\,°$ were assigned to the Fe_3O_4 nanoparticles and the peaks at $2\theta = 38.2\,°$ and $43\,°$ were attributed to highly crystalline silver nanoparticles.

3.3. TEM Analysis

TEM analysis was used to study the existence and dispersion of nanoparticle within the structure of the nanocatalyst. The TEM image of Ag/Fe_3O_4@starch confirmed the existence of the nanoparticles in the starch with a diameter below 10 nm (Fig. 3). Also, good dispersity and monodispersity of nanoparticles in the starch matrix are shown in this TEM image.

3.4. TGA Analysis

The thermal stability of Ag/Fe_3O_4@starch was examined *via* TGA. TGA analysis of the Ag/Fe_3O_4@starch nanocomposite is shown in Fig. 4. Minor weight loss 30–130 °C was assigned to the loss of adsorbed water (4.7 %). The large weight loss between 250 and 600 °C was owing to the decomposition of starch (52.3 %). The TGA/DTA curve of the Ag/Fe_3O_4@starch as shown in Fig. 4; indicates the removal of adsorbed water and organic solvents.

3.5. EDX Analysis

EDX analysis was performed for the elemental analysis of Ag/Fe_3O_4@starch. The patterns (Fig. 5) showed that the nano-

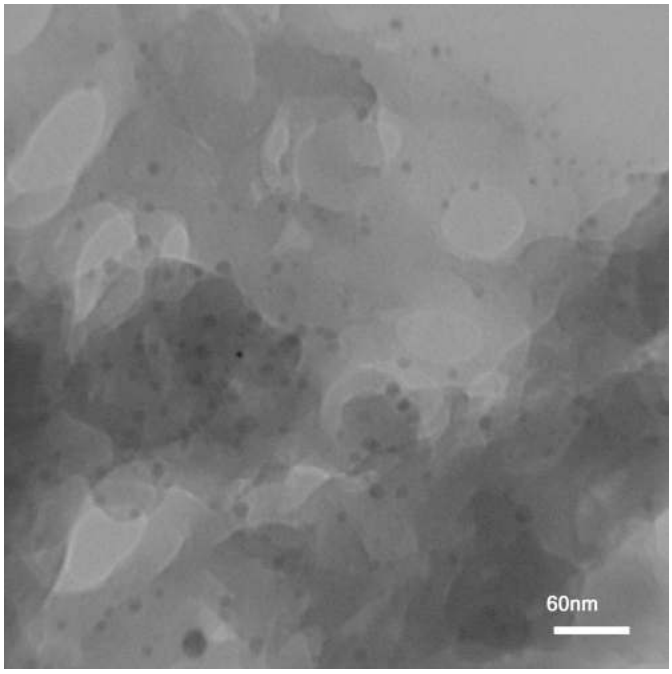

Figure 3 TEM image of Ag/Fe_3O_4@starch.

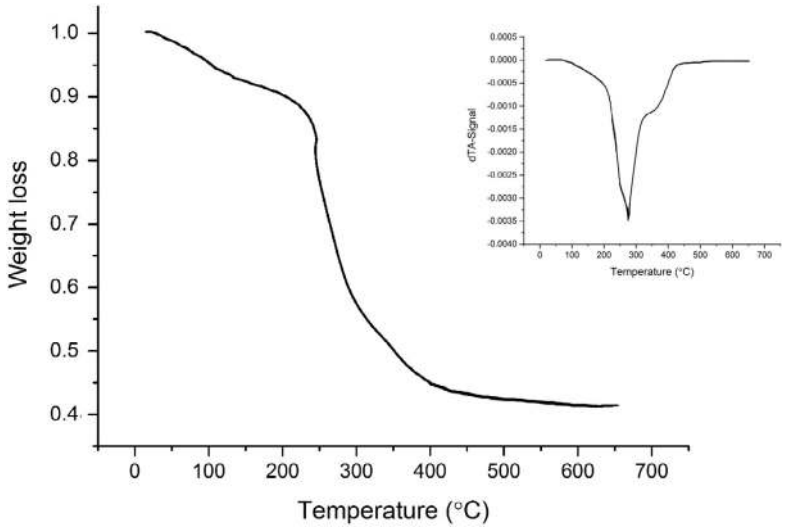

Figure 4 TGA of Ag/Fe_3O_4@starch.

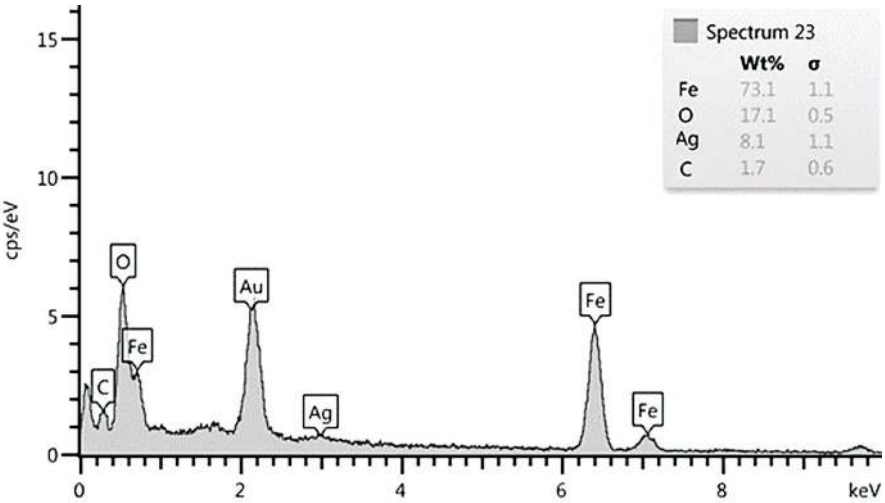

Figure 5 EDX spectrum of Ag/Fe_3O_4@starch nanocomposite.

composite contains Fe, Ag, O and C, which was well-matched with elements of the precursors. The loading of silver supported on the starch was found to be 5.2 wt. % based on the results gained from the atomic absorption spectroscopy.

3.6. VSM Analysis

Ag/Fe_3O_4@starch were simply attracted to an external magnet which showed the formation of magnetic NPs. In addition to the aforementioned simple test, the magnetic property of the Ag/Fe_3O_4@starch was measured by a VSM at room temperature (Fig. 6). The saturation magnetization (Ms) and the coercivity (Hc) of Ag/Fe_3O_4@starch were about 22.37 emu g^{-1} and 6.3 Oe, respectively. The ease in separation and recycling of Ag/Fe_3O_4@starch used as a catalyst in the reaction was owing to the obtained high magnetic saturation.

3.7. Using of the Nanocatalyst in the 4*H*-pyrans and Tetrahydro-4*H*-chromenes Synthesis

The catalytic activity of Ag/Fe_3O_4@starch for the formation of 4*H*-pyrans and tetrahydro-4*H*-chromenes was evaluated. In a preliminary investigation, the one-pot, three-component reaction of benzaldehyde (**1a**), malononitrile (**2**) and dimedone (**3d**) in a molar ratio (1:1:1) in absence of any catalyst did not lead to the desired product **4p** and even increasing the reaction times did not improve the yield (Table 1, entry 1). Several, tests were conducted to optimize the reaction conditions including solvent ($CHCl_3$, EtOH, H_2O and H_2O/EtOH) and the catalyst (starch, Fe_3O_4@starch, Ag@starch, and Ag/Fe_3O_4@starch), all parameters of which are summarized in Table 1. To optimize the reaction temperature, the model reaction was carried out at different temperatures ranging from room temperature to 80 °C. Moreover, it was observed that, in the presence of starch, Fe_3O_4@starch, or Ag@starch up to 79 % yield of compound **4p** was achieved after 10 min (Table 1, entries 2–4). The maximum yield (95 %) was in the presence of Ag/Fe_3O_4@starch 20 mg and ethanol as solvent at 50 ºC in 10 min (Table 1, entry 16).

To evaluate catalyst loading in the model reaction, the procedure was optimized using Ag/Fe_3O_4@starch which afford the product at a range of trace-95 % yield (Table 1, entries 11–17). High yields (92 %) of product **4p** was achieved using 15 mg of Ag/Fe_3O_4@starch as a nanocatalyst in EtOH after 10 min of reaction time (Table 1, entry 15).

In contrast, low amounts of catalyst led to moderate outcomes of the product at longer reaction times; also, using larger amounts of Ag/Fe_3O_4@starch had no significant effect on the yields (Table 1, entry 15 *vs* entry 16). The yield plateaued when the temperature was further increased to 80 °C. Therefore, the most suitable reaction temperature is 50 °C. These results showed that Ag/Fe_3O_4@starch is an essential agent in promoting the reaction.

After optimizing the reaction conditions, this sustainable protocol was next successfully tested in producing **4a–t** in high to excellent yields (84 to 95 %) and short reaction times (9–17 min) in EtOH, by employing of a series of different aldehydes, 1,3-diketoesters [such as methyl acetoacetate (**3a**) and ethyl acetoacetate (**3b**)] or cyclic 1,3-diketones [such as cyclohexane-1,3-dione (**3c**) and dimedone (**3d**)] and malononitrile. Upon, completion of the reaction, the nanocatalyst was simply recovered by an external magnet, washed with ethanol, and reused directly with fresh reagents under the same conditions without the loss of activity. A summary of the experimental details including the substrate, product, reaction times, melting point, and yield of all target compounds are listed in Table 2. Moreover, the melting points were compared to the known products reported in the literature.

The proposed mechanism of reaction shows the influence of the nanocatalyst on the formation of products as illustrated in Scheme 1. The Knoevenagel condensation of activated aryl

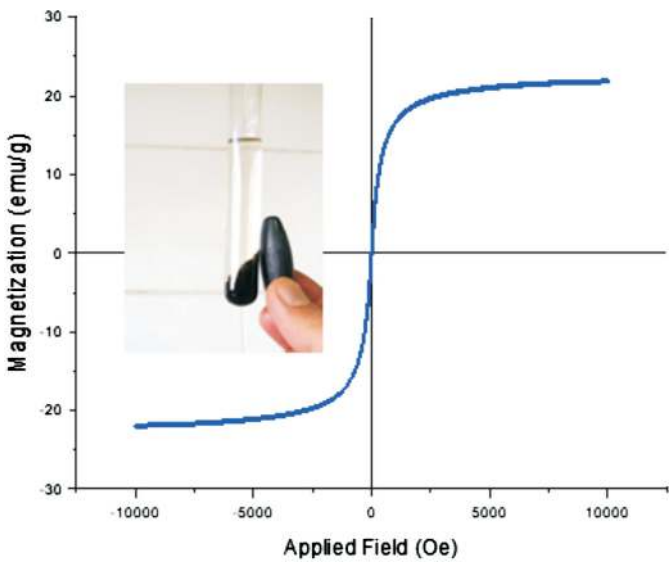

Figure 6 Magnetization hysteresis curve of Ag/Fe_3O_4@starch.

Table 1 Effect of different parameters on the synthesis of compound **4p** as a trial reaction.[a]

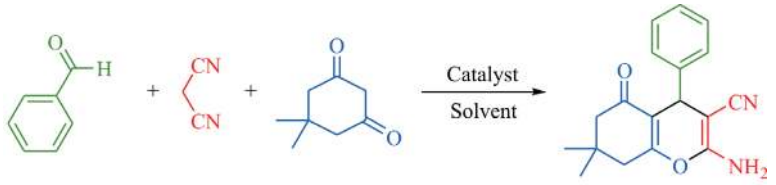

Entry	Catalyst/mg	Solvent	Temperature/°C	Time/min	Yield[b]/%
1	–	EtOH	50	10	–
2	Starch (20)	EtOH	50	10	Trace
3	Fe_3O_4@starch (20)	EtOH	50	10	30
4	Ag@starch (20)	EtOH	50	10	79
5	Ag/Fe_3O_4@starch (20)	–	RT	10	–
6	Ag/Fe_3O_4@starch (20)	–	80	20	–
7	Ag/Fe_3O_4@starch (20)	H_2O	80	10	–
8	Ag/Fe_3O_4@starch (20)	$CHCl_3$	50	10	88
9	Ag/Fe_3O_4@starch (20)	CH_3CN	50	10	50
10	Ag/Fe_3O_4@starch (20)	H_2O/EtOH	60	30	25
11	Ag/Fe_3O_4@starch (1)	EtOH	50	10	Trace
12	Ag/Fe_3O_4@starch (5)	EtOH	50	10	61
13	Ag/Fe_3O_4@starch (8)	EtOH	50	10	70
14	Ag/Fe_3O_4@starch (10)	EtOH	50	10	78
15	**Ag/Fe_3O_4@starch (15)**	**EtOH**	**50**	**10**	**92**
16	Ag/Fe_3O_4@starch (20)	EtOH	50	10	95
17	Ag/Fe_3O_4@starch (30)	EtOH	50	10	88

[a] Reaction was performed with benzaldehyde (**1a**, 1 mmol), malononitrile (**2**, 1 mmol), dimedone (**3d**, 1 mmol), and catalyst.
[b] Isolated yield.
' – ' indicates no reaction. RT: room temperature. The bold type (entry 15) refers to the best reaction conditions.

aldehydes **1** with malononitrile (**2**) form intermediate cyano-olefines **I.** The Michael type addition of activated 1,3-diketo-esters or cyclic 1,3-diketones **3** to the intermediate **I** give the intermediate **II**, which intramolecular cyclization produce the final products **4**. In this method, Ag/Fe_3O_4@starch plays a crucial role in accelerating all stage of the reaction.

The behaviour, usefulness, and capability of Ag/Fe_3O_4@starch system for the formation of product **4p** were highlighted by a comparison of the results obtained with other reported systems, as shown in Table 3. As is evident from Table 3, our procedure in the presence of Ag/Fe_3O_4@starch as a nanocatalyst shows a greater or comparable efficiency such as short reaction times, using cheap and eco-friendly materials, and also simple magnetic recoverability compared with the other systems in the literature.

3.8. Catalyst Recycling

Furthermore, the recoverability of Ag/Fe_3O_4@starch as a key factor of a catalytic system was also studied for the synthesis of product **4p**. To this end, the catalyst was simply separated from the reaction mixture using an external magnet, recovered and reused for up to five sequential runs with an average efficiency of 90 % without any loss of activity (Fig. 7).

4. Conclusions

In this study, Ag/Fe_3O_4@starch was synthesized and used as a magnetic nanocatalyst, and it was characterized by XRD, EDX, VSM, FT-IR, TEM and TGA. Also, to examine the application of the nanocatalyst, it was used as a heterogeneous nanocatalyst for one-pot synthesis of 4*H*-pyrans and tetrahydro-4*H*-chromenes with 84–95 % substance yields, that are frequently applied as pharmacologically and biologically active products, *via* a three-component condensation of aryl aldehydes, malononitrile and 1,3-diketoesters or cyclic 1,3-diketones in the presence of ethanol at 50 °C. The prepared magnetic nanocatalyst was separated from the reaction mixture by a bar magnet, demonstrating its use as a recyclable nanocatalyst. Some of the considerable advantages of this inexpensive, new catalyst, are its low loading, simple recoverability, short reaction times, and high yields of the products resulting in an efficient and environmentally friendly procedure.

Acknowledgement

The authors are grateful for the support provided by Urmia University.

[§]ORCID iD

A. Poursattar Marjani: orcid.org/0000-0002-5899-4285

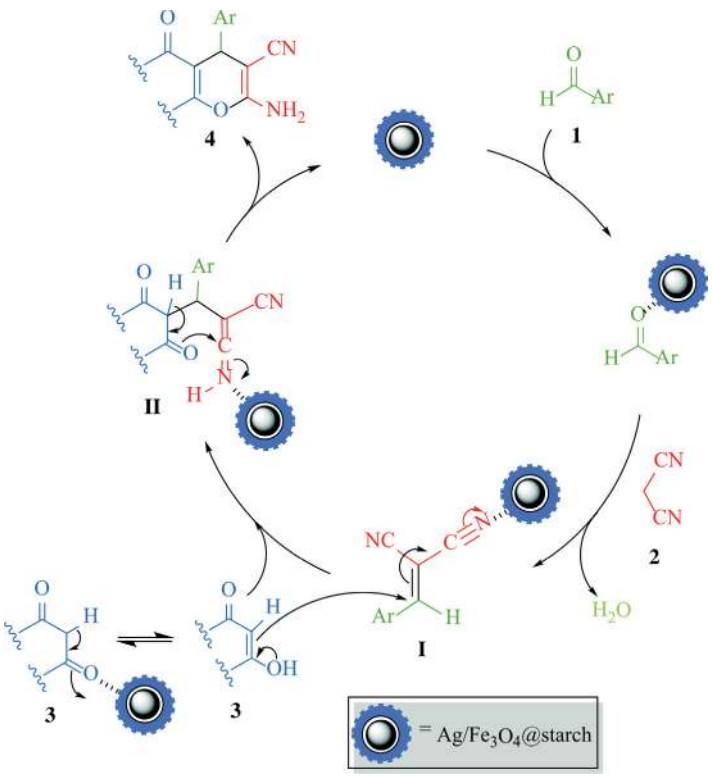

Scheme 1
A plausible mechanistic pathway for the formation of final products in the presence of magnetic nanocatalyst.

Table 2 The reaction condition, yields and melting points of products **4a–t**.

Entry	Aryl aldehydes	1,3-Diketoesters / Cyclic 1,3-diketones	Products	Time/min	Yield[b]/%	M.p/°C Observed	Reported
1	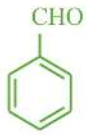	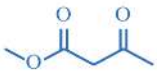	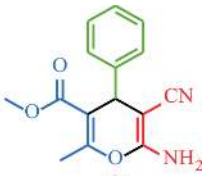 **4a**	14	87	170–173	172–173 [14]
2	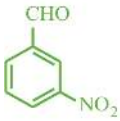	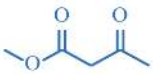	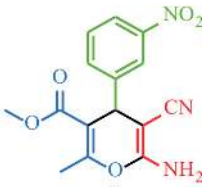 **4b**	16	90	212–214	212–213 [15]
3		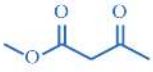	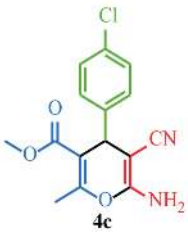 **4c**	17	89	171–173	172–173 [15]
4		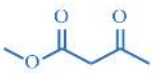	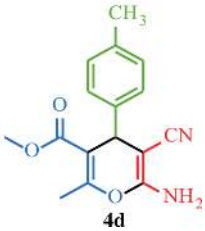 **4d**	13	84	173–175	174–175 [15]

Continued on p. 61

Table 2 (continued)

Entry	Aryl aldehydes	1,3-Diketoesters / Cyclic 1,3-diketones	Products	Time/min	Yield[b]/%	M.p/°C Observed	Reported
5	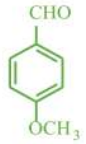	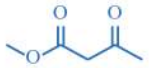	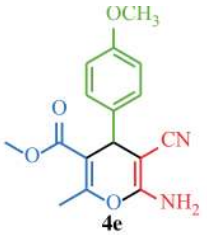 **4e**	15	91	149–152	149–150 [15]
6		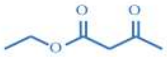	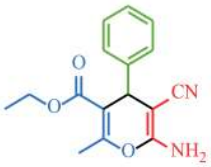 **4f**	9	90	194–196	193–195 [16]
7	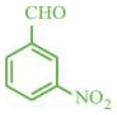	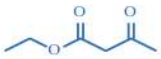	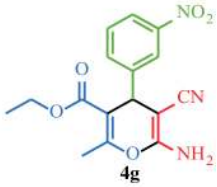 **4g**	11	91	183–186	183–185 [17]
8	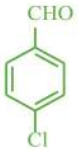	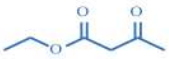	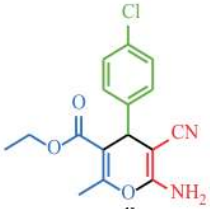 **4h**	8	95	172–174	173–175 [16]
9			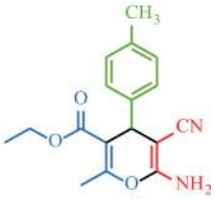 **4i**	15	91	180–183	180–182 [16]
10	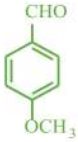		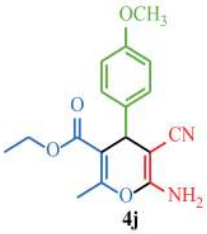 **4j**	16	86	139–142	140–142 [16]
11	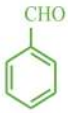	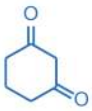	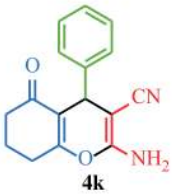 **4k**	10	87	238–240	239–241 [16]
12	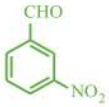	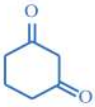	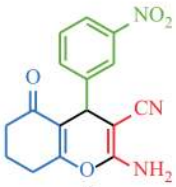 **4l**	12	92	202–205	201–202 [18]

Continued on p. 62

Table 2 (continued)

Entry	Aryl aldehydes	1,3-Diketoesters / Cyclic 1,3-diketones	Products	Time/min	Yield[b]/%	M.p/°C Observed	Reported
13	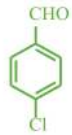	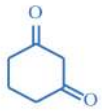	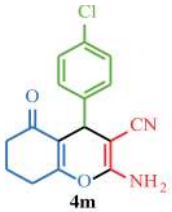 **4m**	9	89	226–228	226–229 [16]
14	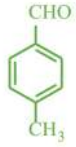	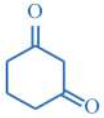	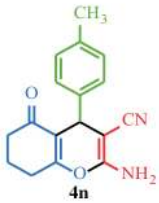 **4n**	14	86	213–215	214–216 [16]
15	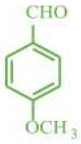	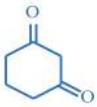	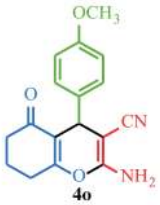 **4o**	13	87	194–197	193–195 [16]
16	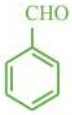	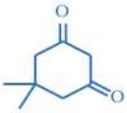	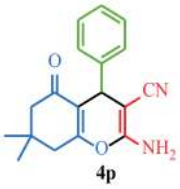 **4p**	11	92	230–232	228–230 [16]
17	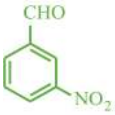	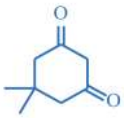	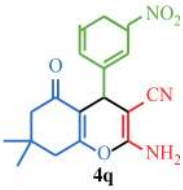 **4q**	10	94	210–212	212–214 [18]
18	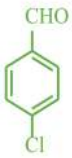	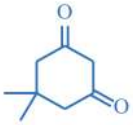	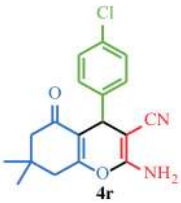 **4r**	12	91	208–211	207–209 [16]
19	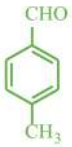	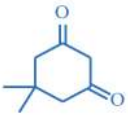	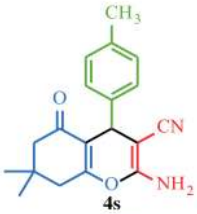 **4s**	13	87	222–225	223–225 [16]
20		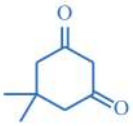	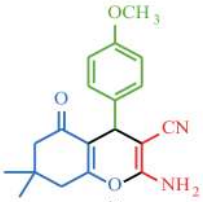 **4t**	15	88	201–203	201–202 [16]

[a] Reaction condition: aryl aldehyde (1 mmol), malononitrile (1 mmol) and 1,3-diketoester or cyclic 1,3-diketone (1 mmol) in 5 mL of ethanol at 50 °C in the presence of 15 mg of nanocatalyst. [b] Yields refer to isolated pure products.

Table 3 Comparison of the activity of different catalysts in the literature to the synthesis of **4p**.

Entry	Catalyst	Temp /°C	Time /min	Yield/%	Ref.
1	MgO	RT	10	75	[19]
2	Nano-SiO_2	70	8	94	[20]
3	Palladium nanoparticles	Reflux	5 h	87	[21]
4	$NH_4Al(SO_4)_2{\cdot}12H_2O$	80	120	92	[22]
5	BF_3OEt_2	Reflux	120	85–90	[23]
6	Fructose	40	45	86	[24]
7	Fe_3O_4@g-C_3N_4	60–80	60	97	[25]
8	α-$Zr(KPO_4)_2$	60	120	93	[26]
9	γ-Al_2O_3	50	10 h	95	[27]
10	ZnO	RT	240	86	[28]
11	Ag/Fe_3O_4@starch	50	11	92	This work

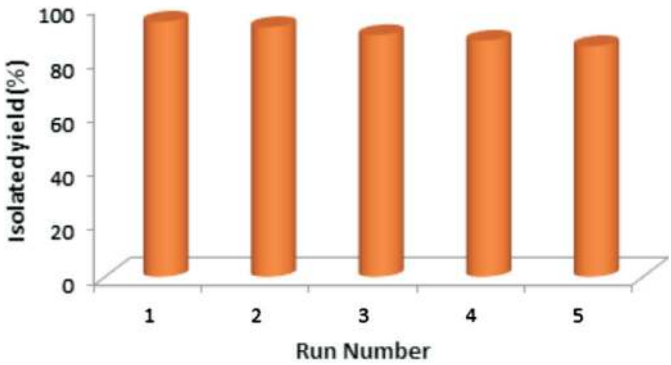

Figure 7 Reusability of nanocatalyst in the synthesis of compound **4p**.

References

1 H. Nosrati, S. Pourmotabed and E. Sharifi, A review on some natural biopolymers and their applications in angiogenesis and tissue engineering, *J. Appl. Biotechnol. Rep.*, 2018, **5**, 81–91.

2 E. Bertoft, Understanding starch structure: recent progress, *Agronomy* 2017, **7**, 56.

3 U. Shah, A. Gani, B.A. Ashwar, A. Shah, M. Ahmad, A. Gani, I.A. Wani, F.A. Masoodi and F. Yildiz, A review of the recent advances in starch as active and nanocomposite packaging films, *Cogent Food Agric.*, 2015, **1**, 1115640.

4 V.V. Makarov, A.J. Love, O.V. Sinitsyna, S.S. Makarova, I.V. Yaminsky, M.E. Taliansky and N.O. Kalinina, "Green" nanotechnologies: synthesis of metal nanoparticles using plants, *Acta Naturae*, 2014, **6**, 35–44.

5 J. Jung, G.M. Raghavendra, D. Kim and J. Seo, One-step synthesis of starch-silver nanoparticle solution and its application to antibacterial paper coating, *Int. J. Biol. Macromol.* 2018, **107**, 2285–2290.

6 D. Lomelí-Marroquín, D.M. Cruz, A. Nieto-Argüello, A.V. Crua, J. Chen, A. Torres-Castro, T.J. Webster and J.L. Cholula-Díaz, Starch-mediated synthesis of mono- and bimetallic silver/gold nanoparticles as antimicrobial and anticancer agents, *Int. J. Nanomedicine*, 2019, **14**, 2171–2190.

7 M. Hazarika, D. Borah, P. Bora, A.R. Silva and P. Das, Biogenic synthesis of palladium nanoparticles and their applications as catalyst and antimicrobial agent, *PLOS ONE*, 2017, **12**, e0184936.

8 Y. Hou and D.J. Sellmyer, *Magnetic Nanomaterials: Fundamentals, Synthesis and Applications.* Wiley-VCH, Weinheim, 2017.

9 J. Govan and Y.K. Gun'ko, Recent advances in the application of magnetic nanoparticles as a support for homogeneous catalysts, *Nanomaterials*, 2014, **4**, 222–241.

10 S. Majidi, F.Z. Sehrig, S.M. Farkhani, M.S. Goloujeh and A. Akbarzadeh, Current methods for synthesis of magnetic nanoparticles, *Artif. Cell. Nanomed. B.*, 2016, **44**, 722–734.

11 a) N. Thomas and S.M. Zachariah, Pharmacological activities of chromene derivatives: an overview, *Asian J. Pharm. Clin. Res.*, 2013, **6**, 11–15. b) M. Costa, T.A. Dias, A. Brito and F. Proença, Biological importance of structurally diversified chromenes, *Eur. J. Med. Chem.*, 2016, **123**, 487–507.

12 a) M. Mamaghani, R.H. Nia, F. Tavakoli and P. Jahanshahi, Recent advances in the MCRs synthesis of chromenes: a review, *Curr. Org. Chem.*, 2018, **22**, 1704–1769. b) A. Poursattar Marjani, B. Ebrahimi Saatluo and F. Nouri, An efficient synthesis of 4*H*-chromene derivatives by a one-pot, three-component reaction, *Iran J. Chem. Chem. Eng.*, 2018, **37**, 149–157. c) A. Poursattar Marjani, J. Khalafy, P. Eslamipour and M. Ahmadi Sabegh, Synthesis of a new series of 4*H*-benzo[*h*]chromenes by a multicomponent reaction under solvent-free microwave conditions, *Iran J. Chem. Chem. Eng.*, 2019, **38**, 51–57.

13 A. Zamani, A. Poursattar Marjani, A. Nikoo, M. Heidarpour and A. Dehghan, Synthesis and characterization of copper nanoparticles on walnut shell for catalytic reduction and C-C coupling reaction, *Inorg. Nano-Met. Chem.*, 2018, **48**, 176–181.

14 M.S. Pandharpatte, K.B. Mulani and N.N.G. Mohammed, Microwave promoted, sodium acetate catalyzed one pot synthesis of poly functionalized 4*H*-pyrans, *J. Chin. Chem. Soc.*, 2012, **59**, 645–649.

15 F. Yi, Y. Peng and G. Song, Microwave-assisted liquid-phase synthesis of methyl 6-amino-5-cyano-4-aryl-2-methyl-4*H*-pyran-3-carboxylate using functional ionic liquid as soluble support, *Tetrahedron Lett.*, 2005, **46**, 3931–3933.

16 M.A. Nasseri and S.M. Sadeghzadeh, A highly active $FeNi_3$–SiO_2 magnetic nanoparticles catalyst for the preparation of 4*H*-benzo[*b*] pyrans and spirooxindoles under mild conditions, *J. Iran Chem. Soc.*, 2013, **10**, 1047–1056.

17 M. Amirnejad, M.R. Naimi-Jamal, H. Tourani and H. Ghafuri, A facile solvent-free one-pot three-component method for the synthesis of 2-amino-4*H*-pyrans and tetrahydro-4*H*-chromenes at ambient temperature, *Monatsh. Chem.*, 2013, **144**, 1219–1225.

18 A. Patra and T. Mahapatra, Synthesis of tetrahydrobenzo[*b*]pyran derivatives catalysed by aliquat®336 in water under microwave irradiation, *J. Chem. Res.*, 2010, **34**, 689–693.

19 D. Kumar, V. Buchi Reddy, S. Sharad, U. Dube and S. Kapur, A facile one-pot green synthesis and antibacterial activity of 2-amino-4*H*-pyrans and 2-amino-5-oxo-5,6,7,8-tetrahydro-4*H*-chromenes, *Eur. J. Med. Chem.*, 2009, **44**, 3805–3809.

20 E. Mollashahi and M. Nikraftar, Nano-SiO_2 catalyzed three-component preparations of pyrano[2,3-*d*]pyrimidines, 4*H*-chromenes, and dihydropyrano[3,2-*c*]chromenes, *J. Saudi Chem. Soc.*, 2018, **22**, 42–48.

21 M. Saha and A.K. Pal, Palladium (0) nanoparticles: a novel and reusable catalyst for the synthesis of various pyran derivatives, *Adv. Nanopart.*, 2012, **1**, 61–70

22 A.A. Mohammadi, M.R. Asghariganjeh and A. Hadadzahmatkesh, Synthesis of tetrahydrobenzo[*b*]pyran under catalysis of $NH_4Al(SO_4)_2{\cdot}12H_2O$ (Alum), *Arab. J. Chem.*, 2017, **10**, S2213–S2216.

23 A. Sethukumar, V. Vithya, C.U. Kumar and A.B. Prakasam, NMR spectral and structural studies on some xanthenones and their thiosemicarbazone derivatives: crystal and molecular structure of 12-(2-chlorophenyl)-8,9,10,12-tetrahydrobenzo[*a*]xanthen-11-one, *J. Mol. Struct.*, 2012, **1008**, 8–16.

24 S.S. Pourpanah, S.M. Habibi-Khorassani and M. Shahraki, Fructose-catalyzed synthesis of tetrahydrobenzo[*b*]pyran derivatives: investigation of kinetics and mechanism, *Chinese J. Cat.*, 2015, **36**, 757–763.

25 N. Azizi, T. Soleymani Ahooie, M.M. Hashemi and I. Yavari, Magnetic graphitic carbon nitride-catalyzed highly efficient construction of functionalized 4*H*-pyrans, *Synlett.*, 2018, **29**, 645–649.

26 O. Rosati, A. Pelosi, A. Temperini, V. Pace and M. Curini, Potassium-exchanged zirconium hydrogen phosphate [α-$Zr(KPO_4)_2$]- catalyzed synthesis of 2-amino-4*H*-pyran derivatives under solvent-free conditions, *Synthesis*, 2016, **48**, 1533–1540.

27 L. Edjlali and R. Hosseinzdeh-Khanmiri, γ-L-CASE-alumina catalyzed green synthesis of pyran's annulated heterocyclic systems via three-component reaction, *Iran J. Sci. Technol. Trans. Sci.*, 2016, **40**, 151–1 56.

28 P. Bhattacharyya, K. Pradhan, S. Paul and A.R. Das, Nano crystalline ZnO catalyzed one pot multicomponent reaction for an easy access of fully decorated 4*H*-pyran scaffolds and its rearrangement to 2-pyridone nucleus in aqueous media, *Tetrahedron Lett.*, 2012, **53**, 4687–4691.